ELSEVIER

Coordination Chemistry Reviews
171 (1998) 461–480

COORDINATION CHEMISTRY REVIEWS

Strategies for enhancing photoluminescence of Nd^{3+} in liquid media

Shozo Yanagida [a,*], Yasuchika Hasegawa [a], Kei Murakoshi [a], Yuji Wada [a], Nobuai Nakashima [b], Tatsuhiko Yamanaka [c]

[a] *Material and Life Science, Graduate School of Engineering, Osaka University, Yamada-oka, Suita, Osaka 565, Japan*
[b] *Department of Chemistry, Faculty of Science, Osaka City University, Osaka, Japan*
[c] *Institute of Laser Engineering, Osaka University, Yamada-oka, Suita, Osaka 565, Japan*

Received 7 July 1997; accepted 19 November 1997

Contents

* Corresponding author. Fax: +81 6 877 9067.

PII S0010-8545(98)00047-2

Abstract

The excited state ($^4F_{3/2}$) of Nd^{3+} readily undergoes radiationless energy transfer via vibrational excitation of surrounding medium and dipole–dipole energy transfer via cross relaxation and energy migration, which makes it difficult to observe luminescence of Nd^{3+} in a liquid matrix. In order to suppress such de-excitation of the $^4F_{3/2}$ state, two kinds of β-diketonato ligands which have no C–H and O–H bonds having high vibrational frequency were successfully designed for observing luminescence of Nd^{3+} in a liquid matrix. Luminescence of Nd^{3+} was observed for the first time by using deuterated tris-(hexafluoroacetylacetonato) neodymium(III), Nd(HFA-D)$_3$, in deuterated organic solvents. The luminescence intensity, lifetime and quantum yield of the complex were measured in methanol-d_4, acetone-d_6, THF-d_8, DMF-d_7 and DMSO-d_6. Deuterated tris(bis-(perfluorooactanoyl) methanato)neodymium(III), Nd(POM-D)$_3$, gave enhanced luminescence in DMSO-d_6 by minimizing energy migration during diffusional collisions in the liquid matrix. The intensity was independent of concentration in the micromolar range from 0.01 to 0.07M. The bulky perfluoroalkyl groups in the ligands effectively prevented de-excitation via vibrational excitation and cross relaxation in liquid media. © 1998 Elsevier Science S.A.

Keywords: Excited state; Energy transfer; Luminescence

1. Introduction

Solid systems containing Nd^{3+} have been regarded as the most popular luminescent materials for laser system applications [1–3]. Since high-power neodymium lasers with output wavelength at around 1.06 μm are of interest in laser inertial confinement experiments, Nd-containing matrices such as oxide, fluoride, phosphate and mixed glass matrices have been investigated for capability of higher power laser radiation under control of Nd^{3+} density in glass matrices. At the Institute of Laser Engineering (ILE), Osaka University, research on laser-induced inertial confinement nuclear fusion has been in progress using an Nd^{3+}-containing phosphate glass laser, GEKKO XII since 1976, and the ILE achieved more than 60 TW as a maximum power of this laser system [4,5]. However, Nd-laser glass systems would have an intrinsic problem of heat destruction under conditions of high-power laser emission with high frequency; repeated operation causes accumulation of heat, resulting in degradation of solid matrices. At the present stage of experimentation using the GEKKO XII system, only one or two operations are allowed in one day (0.0001 Hz). In order to achieve continuous operation for the inertial confinement at a level of practical application (hopefully more than 10 Hz), the system of liquid Nd^{3+}-containing luminescent medium has been considered promising compared with recent progress of semiconductor laser (laser diode) devices. Liquid Nd^{3+}-containing luminescent media could be cooled by circulation, which would enable the laser system to work with high power and high frequency.

From these points of view, we have aimed at developing luminescent materials consisting of Nd^{3+} complexes in liquid organic media. Literature survey revealed that Rusakova and Beeby reported the emission of $Nd(NO_3)^{3+}$ in deuterated DMSO [6–8]. In general, effective luminescence of Nd^{3+} was regarded as almost impossible

in organic solvents, because the emitting level of Nd^{3+} is susceptible to the radiationless transition through vibrational excitation of ligands or solvent molecules. In addition, excitation migration induced by collision between Nd^{3+} was regarded unavoidable in a liquid matrix. Here we present a review of how to control radiationless quenching of emitting states of Nd^{3+} in an organic liquid matrix, i.e. strategies for enhancement of the luminescence by designing ligand and solvent molecules in liquid neodymium complex systems.

2. Theoretical aspects for enhancing luminescence of the Nd^{3+} ion

Absorption and emission processes of Nd^{3+} originate from electronic transition in its f-orbitals. Although the electronic transition in the f-orbitals is forbidden by the selection rule, the perturbation from the surrounding medium makes the f–f transitions allowed, enabling the excited states to emit photons with relatively long lifetimes. Since Nd^{3+} may have metastable excited states under favorable conditions, the formation of a population inversion via "4 level transition" for laser emission of Nd^{3+} becomes possible as illustrated in Fig. 1. As expected, all emissions of Nd^{3+} arising from the $^4F_{3/2}$ state to the various ground states manifolds ^4I_J, $J=$ 15/2, 13/2, 11/2, 9/2. Accordingly, it is necessary to minimize the nonradiative energy transfer from the $^4F_{3/2}$ state. One approach is suppression of radiationless energy transfer via vibrational excitation. Another approach is prevention of energy transfer through cross relaxation and excitation migration during diffusional collisions.

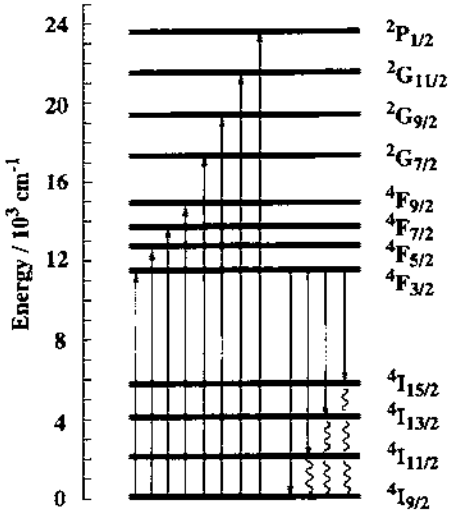

Fig. 1. Absorption and radiative transition of the Nd^{3+} ion.

2.1. Suppression of energy transfer process via vibrational excitation

The energy transfer process via vibrational excitation has been considered as a dominant process which quenches the excited states of Nd^{3+} in solution. The difficulty in enhancing the luminescence of Nd^{3+} in liquid systems is believed to be due to the radiationless relaxation of the emitting level ($^4F_{3/2}$) via vibrational excitation of the liquid matrix consisting of ligand and solvent molecules as shown schematically in Fig. 2(a). The vibrational transition probability is proportional to the Franck–Condon factor, i.e. overlap integrals between the energy gap and vibrational energy. In terms of the energy gap theory, the rate constant for radiationless transition, $W_{\text{Radiationless Transmission}}$, is given by

$$W_{\text{RadiationlessTransition}} = (2\pi\rho/h)J^2F \tag{1}$$

where ρ is the density of state, $J(=\int \phi_i Q \phi_j \, d\tau)$ is the coupling constant between the

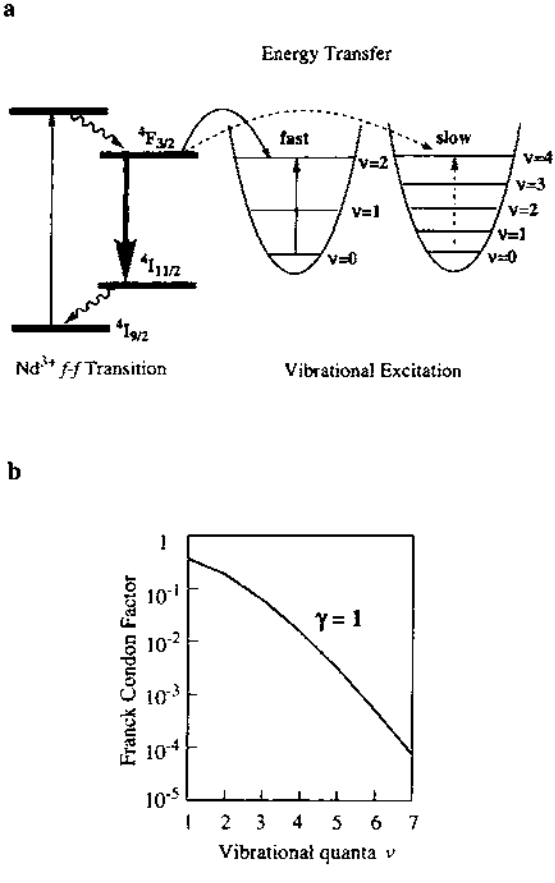

Fig. 2. Radiationless transition via vibrational transition and Franck–Condon factor.

electronic wave functions due to nuclear motion, F is the Franck–Condon factor. The factor F should be estimated quantitatively when an approximation using an undistorted oscillator model is adopted. In the model, F is given by

$$F(E)=\exp(-\gamma)\gamma^{v}/v! \tag{2}$$

$$\gamma=\tfrac{1}{2}k(\vec{q}-\vec{q}^{0})^{2}/\hbar\omega \tag{3}$$

where q and q^0 are the equilibrium positions of the vibrational initial and final states, respectively [9]. If γ is assumed to be 1, the Franck–Condon factor decreases with increase of vibrational quanta v as shown in Fig. 2(b).

The radiative transition in Nd^{3+} occurs at $^4F_{3/2}$. The energy gap of the crucial radiative transition in Nd^{3+} ($^4F_{3/2}\rightarrow{}^4I_{15/2}$: 5400 cm^{-1}) matches well the vibration of C–H and O–H bonds (5900 and 6900 cm^{-1}, respectively) with vibrational quanta $v=2$, and vibrational excitation leads to effective quenching of the excited state of Nd^{3+}. Since conventional organic solvents contain many C–H bonds, de-excitation via vibrational excitation prevails. Accordingly, if the Nd^{3+}-surrounding liquid matrix can be constructed with molecules of larger vibrational quanta ($v\geq 3$), the radiationless transition through vibrational excitation should be suppressed to an appreciable extent. The idea of employing solvent molecules with low energy vibration as a liquid matrix for Nd^{3+} was demonstrated by Heller et al. [10,11] whose work led to the first successful utilization of inorganic aprotic liquid molecules, $SeOCl_2$ and $POCl_3$, for enhanced luminescence of Nd^{3+} in a liquid matrix, and eventually for laser emission [12–17]. However, such unconventional solvents are not appropriate for practical applications because of their high reactivity and toxicity.

While the O–H or C–H bonds are vibrational energy gaps which match the radiative transition at vibrational quanta, $v=2$, O–D, C–D, C–O, C–C and C–F bonds give larger vibrational quanta, $v\geq 3$ (Fig. 3). In theoretical calculations, the

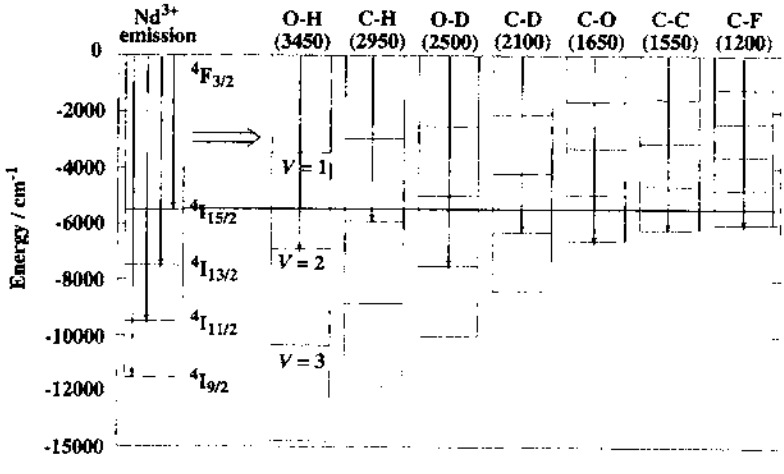

Fig. 3. Schematic presentaiton of the vibrational energy of chemical bonds and their matching with the electronic energy gap of the Nd^{3+} ion.

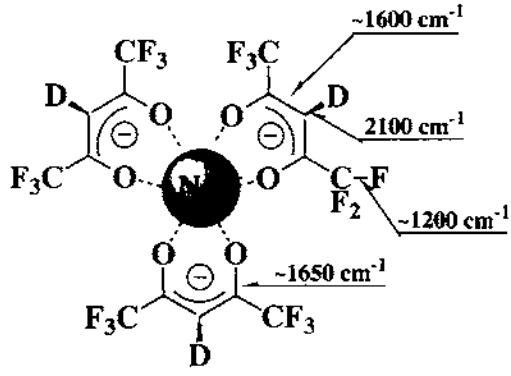

Fig. 4. Chemical structure of tris-(hexafluoroacetylacetonato)neodymium(III), $Nd(HFA\text{-}D)_3$, and vibration wave numbers.

Franck–Condon factors of C–H and C–F are determined to be 0.18 and 0.0031, respectively. These facts suggest that favorable liquid media could be constructed using ligand and solvent molecules with C–D and C–F bonds instead of C–H bonds. This theoretical understanding led to the first successful utilization of deuterated hexafluoraocetylacetone (HFA-D) as an effective ligand, which enabled the resulting Nd complex to exhibit luminescence in an organic liquid matrix (Fig. 4) [18,19].

2.2. Prevention of energy transfer through cross relaxation and excitation migration at diffusion collision

Deactivation of the luminescent states of Nd^{3+} in solution occurs not only via vibrational excitation but also via dipole–dipole energy transfer between neighboring Nd^{3+} complexes. Diffusion of Nd^{3+} complexes in a liquid system induces collisions between the molecules, leading to energy transfer via cross relaxation and excitation migration. As depicted in Fig. 5, these quenching processes are based on a dipole–dipole interaction between the molecules [20,21].

The cross relaxation is a process where the energy of excitation, initially localized on one ion, is partially transferred to a neighboring ion, leaving both ions in lower energy levels that decay rapidly to the ground state. The migration of excited states by hoping does not quench luminescence by itself, but it enhances the probability of quenching by permitting the movement of the excitation to sites where more rapid quenching can take place. The cross relaxation and excitation migration processes are both examples of dipole–dipole energy transfer processes. According to Förster–Dexter theory, the critical distance R_{DX} for nonradiative dipole–dipole energy transfer is given by

$$R_{DX}^{6} = \frac{3c}{8\pi^4 n^2 A_r} \int \sigma_D^{em}(\lambda)\sigma_X^{abs}(\lambda)\,d\lambda \tag{4}$$

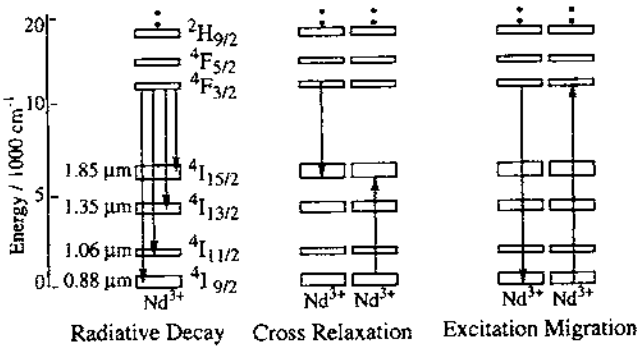

Fig. 5. Three major relaxation processes for the neodymium(III) ion. (a) Radiative decay: the spontaneous emission of photons accompanies transitions from the $^4F_{3/2}$ metastable state to lower-lying energy levels. (b) Cross relaxation: an excited Nd^{3+} ion shares its energy with a neighboring Nd^{3+} ion. (c) Excitation migration: the excitation energy moves from one Nd^{3+} ion to another.

where n, A_r and $\int \sigma_D^{em}(\lambda)\sigma_X^{abs}(\lambda)\,d\lambda$ are the ion density, total spontaneous radiative emission rate and resonance integral, respectively.

The theory indicates that the dipole–dipole energy transfer rate declines inversely with the sixth power of the distance between interacting centers. Typical values of the critical distance for excitation migration ($^4F_{3/2}-{}^4I_{9/2}$) and cross-relaxation ($^4F_{3/2}-{}^4I_{15/2}$ and $^4I_{15/2}-{}^4I_{9/2}$) processes in the system of Nd^{3+}-containing phosphate laser glass were estimated to be 11.14 and 4.07 Å, respectively.

The average rates for the energy transfer processes depicted in Fig. 5 should increase rapidly as the Nd^{3+} concentration increases. This reduced luminescence efficiency at high concentration is known as concentration quenching. In order to enhance emission efficiency in liquid systems, we sought to prevent the energy transfer quenching to an appreciable extent even when collision occurs frequently in the liquid systems. In accord with our theoretical understanding of dipole–dipole energy migration, we successfully designed deuterated bis-(perfluorooctanoylmethane) (POM) which exhibited luminescence of the Nd^{3+} complex in a liquid matrix (Fig. 6) [22].

3. Luminescence of Nd(HFA-D)$_3$

We successfully observed luminescence of the neodymium(III) ion (Nd^{3+}) in some deuterated organic solvents using deuterated hexafluoroacetylacetonato

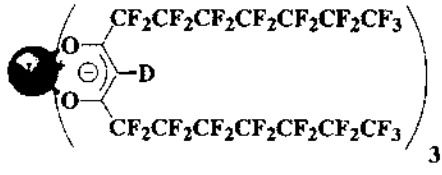

3

Fig. 6. Chemical structures of Nd(POM-D)$_3$.

(HFA-D) as complexing ligands of Nd^{3+} (Fig. 4). The physical nature of the Nd^{3+} coordination environment of the system was compared with that of the Nd^{3+} ion in solid luminescent materials such as Nd^{3+}-containing crystals, Nd:YAG and Nd^{3+}-containing phosphate glass, LGH-8.

3.1. Characteristics of Nd(HFA-D)$_3$

Hexafluoroacetylacetone (HFA) was chosen as a promising ligand because it has only one C–H bond, which is readily replaced by a C–D bond. The structure of the $Nd(HFA)_3$ complex was reported to be a square-antiprism with eight coordinated oxygens of three HFA ligands and two waters of crystallization [23–25]. In fact, DSC analysis of the complex ($Nd(HFA\text{-}H)_3 \cdot 2H_2O$) gave two endothermic peaks at 132.5 and 163.2 °C due to elimination of water molecules of crystallization followed by an endothermic peak at 243.5 °C, the melting point. To eliminate water of crystallization and to replace the C–H bond with C–D bonds, the Nd complex was treated with methanol-d_1 and methanol-d_4 for deuteration using keto–enol equilibrium. The resulting deuterated Nd complex ($Nd(HFA\text{-}D)_3$) is soluble in various organic solvents such as methanol, pyridine, acetonitrile, DMSO, THF, DMF, ether and acetic acid. In particular, acetone gave an extremely high concentration of more than 2M. With this fact in mind, acetone-d_6 was chosen as the solvent for optical measurements of $Nd(HFA\text{-}D)_3$.

3.2. First observation of luminescence of the neodymium(III) ion in acetone-d_6

A solution of $Nd(HFA\text{-}D)_3$ in acetone-d_6 showed emissions at 880, 1062 and 1345 nm when the system was excited at 585 nm (Fig. 7). The quantum yield of the luminescence was determined to be on the order of 10^{-3} using an integral sphere [26,27]. No photoluminescence was observed in either non-deuterated acetone or

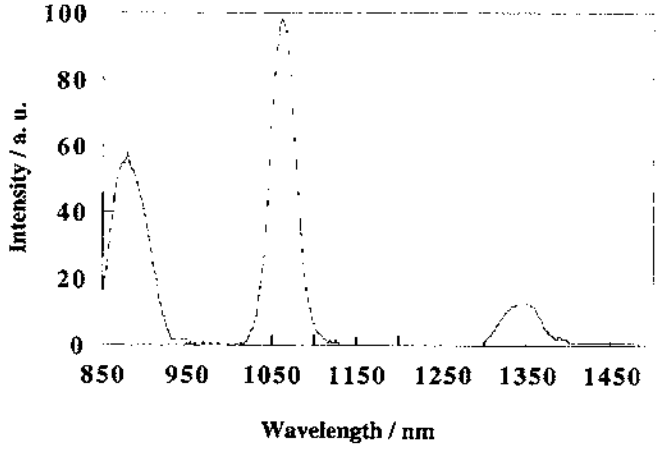

Fig. 7. Emission spectrum of $Nd(HFA\text{-}D)_3$ in acetone-d_6 (conc. 2M).

deuterated acetone without careful dehydration of the system. The quantum yield of the system containing C–H or O–H bond vibrations was estimated to be on the order of 10^{-5}. Spectral peaks at 880, 1062 and 1345 nm were attributed to the f–f transitions $^4F_{3/2} \rightarrow {}^4I_{9/2}$, $^4F_{3/2} \rightarrow {}^4I_{11/2}$ and $^4F_{3/2} \rightarrow {}^4I_{13/2}$, respectively. The emission band at 1062 nm is important because it is potentially applicable for laser emission. Interestingly, it has a symmetrical and narrow structure as is observed for the luminescence of Nd:YAG. It is said that the luminescence from Nd^{3+} in glass matrices shows a relatively wide emission with multiple components due to the various environments of Nd^{3+} in amorphous solid matrices. The band shape with a highly symmetrical structure and relatively narrow width suggests that the environment of Nd^{3+} in Nd(HFA-D)$_3$ could be uniform in the solution system. The energy gap law indicates that the harmonic matching number of the vibrational quanta should be larger than that of O–H and C–H vibrations (3450 and 2950 cm^{-1}). HFA-D ligands in Nd(HFA-D)$_3$ molecules have vibrations of C–F stretching at 1200 cm^{-1} and C–D stretching at 2100 cm^{-1}, and O–D stretching at 2500 cm^{-1}. Absence of C–H and O–H vibrations led to the observation of luminescence from Nd^{3+} in organic solvents. We believe this is the first observation of effective luminescence of Nd^{3+} in organic solvents.

3.3. Effect of coordination structures of Nd(HFA-D)$_3$ on luminescence

3.3.1. Effect of water in the coordination sphere

The quantum efficiency of 0.1M Nd(HFA-D)$_3$ in acetone-d_6 was on the order of 10^{-3}, and the energy transfer via vibrational excitation of surrounding media must still participate in the quenching process. The coordination number of rare earth ions in solution is known to vary from eight to ten depending on the nature of ligating molecules [23–25]. The Nd(HFA-D)$_3$ complex was prepared from Nd(HFA-H)$_3 \cdot (H_2O)_2$ and CD_3OD. Since HFA-D ligands occupy six coordination sites of Nd(HFA-D)$_3$, D_2O molecules may coordinate to the unoccupied sites. The quenching via vibrational excitation of D_2O should be responsible for the still-low emission efficiency, because the probability of energy transfer to the D_2O (2500 cm^{-1}) vibration can be estimated to be quite high. Accordingly, it should be possible to enhance the emission by replacing D_2O in the vicinity of Nd(HFA-D)$_3$ with deuterated solvent molecules having lower vibrational modes (Fig. 8).

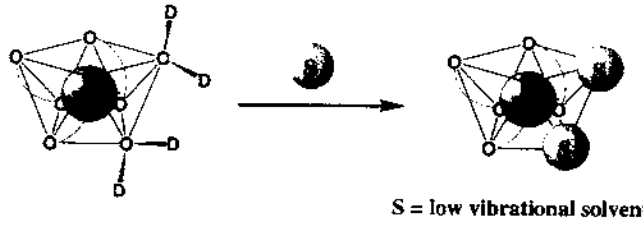

Fig. 8. Suppression of energy transfer quenching via vibrational excitation by replacing coordinated D_2O molecules by low vibrational solvent molecules.

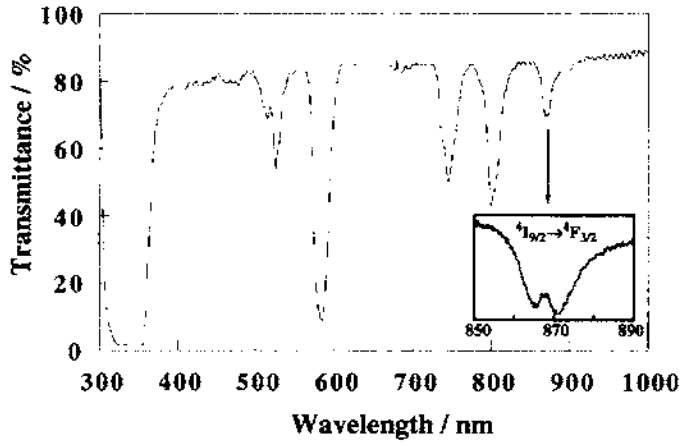

Fig. 9. Transmittance spectra of 0.4 mol m^{-3} [Nd(HFA-D)$_3$] in acetone-d_6. Insert is $^4I_{9/2}\rightarrow{}^4F_{3/2}$ (ground state to emitting level) transmissions spectra.

3.3.2. *Near IR analysis of coordination*

Fig. 9 shows the absorption spectrum of 0.4M Nd(HFA-D)$_3$ in acetone-d_6. Absorption bands were observed at 513, 524, 582, 680, 745, 800 and 865 nm and attributed to the Nd^{3+} transitions of $^4I_{9/2}$ (ground state)→ $^2G_{11/2}$, $^4I_{9/2}\rightarrow{}^2G_{9/2}$, $^4I_{9/2}\rightarrow{}^2G_{7/2}$, $^4I_{9/2}\rightarrow{}^4F_{9/2}$, $^4I_{9/2}\rightarrow{}^4F_{7/2}$, $^4I_{9/2}\rightarrow{}^4F_{5/2}$ and $^4I_{9/2}\rightarrow{}^4F_{3/2}$, respectively. The adsorption spectrum is quite comparable to that of Nd:YAG. The broad absorption band at 320–350 nm is explained as due to ligand HFA-D molecules.

One of the important characteristics of the spectrum is a splitting of the peak at 865 nm as shown in the inset of Fig. 9. The band peak at 865 nm is attributed to the transition $^4I_{9/2}\rightarrow{}^4F_{3/2}$. Thus, the observed splitting indicates that the degenerate $^4F_{3/2}$ level, i.e. the emitting level, splits slightly into two levels. Slight splitting of the $^4F_{3/2}$ degenerate levels should be induced by change in the ligand field around Nd^{3+}.

Table 1 summarizes the splitting energy of the Nd^{3+} ion states in Nd(HFA-D)$_3$, Nd:YAG and LHG-8. The splitting energy of the Nd(HFA-D)$_3$ $^4F_{3/2}$ states, 82.3 cm^{-1}, is similar to that of Nd:YAG (84 cm^{-1}) [28]. On the other hand, LHG-8 Nd^{3+}-containing glasses have a splitting (101.9 cm^{-1}) which is larger than that of Nd(HFA-D)$_3$ and Nd:YAG. LHG-8 is an amorphous glass, and does not have a

Table 1
Splitting energy of emitting level in Nd^{3+}

Compound	$^4F_{3/2}$ (nm)		Splitting energy (cm^{-1})
Nd^{3+}:YAG	868.1	874.5	84
LHG-8	865.5	873.2	101.9
Nd(HFA-D)$_3$	864.8	871.2	82.3

symmetrical structure, whereas Nd:YAG is a pure crystal with the garnet structure. The splitting width observed for the absorption of Nd:YAG can be explained in terms of the characteristics of the crystal structure of the matrix [28]. The comparable splitting width observed for the absorption of $Nd(HFA\text{-}D)_3$ in liquid media with respect to that of Nd:YAG suggests that the field due to the oxygens of the ligand molecules should be similar to that of Nd:YAG. Nd^{3+} in $Nd(HFA\text{-}D)_3$ should be coordinated to eight oxygen atoms which are in three ligand molecules and two solvent molecules, resulting in a strong ligand-field perturbation similar to that in Nd:YAG.

The similarity of the absorption spectra to that of Nd:YAG, suggests that the electronic structure of the Nd^{3+} in the present system should be comparable with that of Nd^{3+} in Nd:YAG.

3.3.3. *NMR analysis of coordination*

In order to elucidate the coordination structures of $Nd(HFA)_3$ in solution, we carried out ^{13}C and ^{19}F NMR measurements. Chemical shifts of carbonyl carbon atoms and trifluoromethyl carbon atoms were obtained, and their relative difference (ΔE) was determined by comparison with that of the free ligand (Table 2). Down field shifts due to the coordination were observed in the system. The shifts should depend on the strength of interaction between Nd^{3+} and the ligand molecule. ΔE values of carbonyl carbon atoms and trifluoromethyl carbon in acetone-d_6 are comparable with those in THF-d_8. ΔE values in DMF-d_7 were smaller than those in acetone-d_6 and THF-d_8. ΔE values in DMSO-d_6 were much smaller than ΔE in other solvents. This is also true for the relative difference (ΔE) in ^{19}F NMR spectra (Table 3).

These results suggest that the coordination structure of the Nd complex depends on the solvent. The difference in ΔE among the solvents reflects the coordination strength between HFA and Nd^{3+}. When solvent molecules coordinate to Nd^{3+}, the chemical shifts in HFA should become small. Shifts in signals of ^{13}C and ^{19}F NMR of the ligand can be a measure of the donation effect of solvent molecules. The

Table 2
^{13}C NMR chemical shifts of hexafluoroacethylacetone (HFA) and tris-(hexafluoroacetylacetonato)neodymium(III) ($Nd(HFA)_3$) in solvents

Solvent	Chemical shift δ in ^{13}C NMR (ppm)[a]					
	^{13}CO of HFA	^{13}CO of $Nd(HFA)_3$	^{13}CO of ΔE[b]	$^{13}CF_3$ of HFA	$^{13}CF_3$ of $Nd(HFA)_3$	$^{13}CF_3$ of ΔE[b]
Acetone-d_6	173.92	187.77	13.85	117.85	150.71	32.96
THF-d_8	173.24	192.37	19.13	118.04	152.71	34.67
DMF-d_7	171.52	180.61	9.09	119.14	114.01	24.87
DMSO-d_6	170.73	174.23	3.50	117.96	132.41	14.45

[a] The ^{13}C NMR chemical shifts were determined using tetramethylsilane (TMS) as an internal standard.
[b] ΔE = (signal position of $Nd(HFA)_3$) − (signal position of HFA).

Table 3
^{19}F NMR chemical shifts of hexafluoroacethylacetone (HFA) and tris-(hexafluoroacetylacetonato) neodymium(III) ($Nd(HFA)_3$) in solvents

Solvent	Chemical shift δ in ^{19}F NMR (ppm)[a]		
	$C^{19}F_3$ of HFA	$C^{19}F_3$ of $Nd(HFA)_3$	$C^{19}F_3$ of ΔE[b]
Acetone-d_6	−74.91	−72.80	2.11
THF-d_8	−75.32	−73.17	2.15
DMF-d_7	−74.70	−74.35	0.35
DMSO-d_6	−75.05	−74.99	0.06

[a] ^{19}F NMR data were determined using hexafluorobenzene as an external standard.
[b] ΔE = (signal position of $Nd(HFA)_3$) − (signal position of HFA).

small ΔE values in DMSO-d_6 suggest that DMSO-d_6 molecules should interact strongly with Nd^{3+} of $Nd(HFA\text{-}D)_3$ in DMSO-d_6.

The ability of the solvent molecules to coordinate to metal centers can be estimated from the donor number (Table 4). The order of donor numbers follows the same trend as the decrease in ΔE values in NMR measurements. Coordination of these solvent molecules is known to take place via oxygen atoms, thus the coordination strength depends on the electron density at the oxygen atoms. Electron densities of oxygen atoms in the solvent molecules, calculated using a MOPAC system (the MNDO/PM3 method), are listed with donor number in Table 4.

The localization of electrons on the oxygen atom in DMSO is significant compared with other solvent molecules. The strong coordination of DMSO molecules confirmed by NMR is in agreement with the negatively charged oxygen of DMSO molecules.

3.3.4. Solvent effect on luminescence

The effect of solvent molecules on the luminescence properties of $Nd(HFA\text{-}D)_3$ was investigated using methanol-d_4, acetone-d_6, THF-d_8, DMF-d_7 and DMSO-d_6. The emission lifetime and quantum yield of $Nd(HFA\text{-}D)_3$ were determined in each solvent. The relationship between the emission characteristics can be understood in terms of solvated molecular structures of $Nd(HFA\text{-}D)_3$ in the various solvents.

Table 4
Donor numbers and calculation of charge distribution of heteroatoms for various solvents

Solvent	Donor number	Charge distribution[a]
Acetone	17.0	−0.2793
THF	20.0	−0.3277
Water	18.0	−0.3291
DMF	26.6	−0.4363
DMSO	29.8	−0.7068

[a] Calculated by MOPAC Ver. 6.10 (MNDO/PM3) program using the CAChe system.

Emission intensity due to the $^4F_{3/2} \rightarrow {}^4I_{11/2}$ transition depends on the choice of solvent. The intensity of the band in DMSO-d_6 was larger by about one order of magnitude than that in methanol-d_4 (Table 5). The emission spectrum of Nd(HFA-D)$_3$ in DMSO-d_6 is shown in Fig. 11(d). The emission spectrum had a symmetrical shape with narrow band width. Full width at half maximum (FWHM) of the emission at 1.06 μm (in DMSO-d_6) was 31.2 nm. Solutions of Nd(HFA-D)$_3$ in acetone-d_6, THF-d_8, DMF-d_7 or methanol-d_4 also gave similar emission spectra. Interestingly, the FWHM depended on the solvent employed (Table 1). The FWHM of [Nd(HFA-D)$_3$] spectra were narrower than that of LHG-8 (35 nm) where Nd^{3+} is surrounded by a glass matrix, and were comparable with that of Nd:YAG (30 nm). The quantum yields of the luminescence in each deuterated solvent are summarized with the emission intensities in Table 5.

The emission decay was also measured (Fig. 10). The inset of Fig. 10 shows a decay profile of the DMSO-d_6 system on a linear scale. The intensity rose within 1 μs, and then decayed exponentially. The lifetimes of the emission, determined by the slope in logarithmic plots of the profile (Fig. 10), are summarized in Table 6. Nd(HFA-D)$_3$ in methanol-d_4 showed the shortest lifetime, 0.70 μs, and the lifetimes in acetone-d_6, THF-d_8 and DMF-d_7 were 1.71, 2.33 and 2.86 μs, respectively. The lifetime of Nd(HFA)$_3$ in DMSO-d_6 was determined to be 6.30 μs, which was the longest among the observed lifetimes. The quantum efficiency increased in the order: methanol-d_4 < acetone-d_6 < THF-d_8 < DMF-d_7 < DMSO-d_6, which agrees well with the order of the emission lifetimes. This agreement suggests that the effective emission in such deuterated solvents should be due to suppression of the nonradiative relaxation processes for Nd^{3+}. Anhydrous DMSO-d_6 was found to be the solvent which gave the strongest emission of Nd(HFA-D)$_3$ in the liquid system.

The characteristics of the luminescence in DMSO cannot be explained only by the difference of the vibrational wave numbers of solvents. The dominant vibrational frequency of DMSO ($\nu_{S=O} = 1060\ cm^{-1}$) is comparable with that of THF ($\nu_{C-O-C} = 1070\ cm^{-1}$). In spite of the similarity in the vibration frequency between DMSO and THF molecules, the emission efficiency in DMSO was found to be much higher than that in THF. The solvent dependence of the emission efficiency, which

Table 5
Characteristics of the emission due to $^4F_{3/2} \rightarrow {}^4I_{11/2}$ transition of Nd(HFA)$_3$ in deuterated solvents

Solvent	Peak wavelength (nm)	FWHM (nm)	Relative intensity[a]	Lifetime (μs)[b]	Φ (%)[c]
Methanol-d_4	1063	33.3	1.0	0.70	~0.1
Acetone-d_6	1055	32.9	1.34	1.71	0.2 (0.4)
THF-d_8	1059	32.0	1.97	2.33	0.3 (0.5
DMF-d_7	1059	30.6	3.00	2.86	0.3 (0.6)
DMSO-d_6	1063	31.2	10.6	6.30	0.6 (1.1)

The quantum yields of the emission in non-deuterated solvents were determined to be in the order of less than 10^{-5}.

[a] Relative intensity was determined from the intensity of the system using methanol-d_4 as a reference.

[b] Excitation at 532 nm.

[c] Excitation at 585 nm. Values in the parentheses are total quantum yields ($^4F_{3/2} \rightarrow {}^4I_{9/2}$, $^4F_{3/2} \rightarrow {}^4I_{11/2}$ and $^4F_{3/2} \rightarrow {}^4I_{13/2}$).

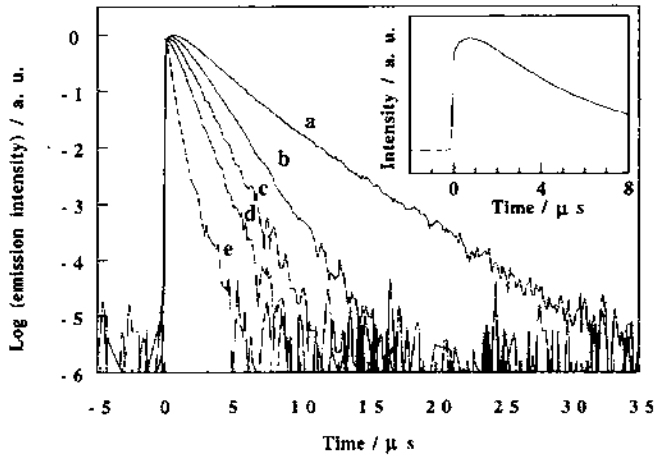

Fig. 10. Emission decays profile in logarithmic scale of 0.1 mol m^{-3} [Nd(HFA-D)$_3$] in (a) DMSO-d_6, (b) DMF-d_7, (c) THF-d_8, (d) acetone-d_6 and (e) methanol-d_4. Insert is emission decays of 0.1 mol m^{-3} Nd(HFA-D)$_3$ in DMSO-d_6.

Table 6
Characteristics of the emission due to $^4F_{3/2} \rightarrow {}^4I_{11/2}$ transition of Nd^{3+} complexes in deuterated DMSO[a]

Complex	Peak wavelength (nm)	FWHM (nm)	Relative intensity	Lifetime (μs)[b]	Φ (%)[c]
Nd(HFA-D)$_3$	1063	31	1.0	6.3	1.3
Nd(POM-D)$_3$	1049	25	2.2	14.5	3.2

[a] The sample concentrations were 0.05 mol m^{-3}. Excitation at 585 nm.
[b] Excitation at 532 nm.
[c] Values were total quantum yield ($^4F_{3/2} \rightarrow {}^4I_{9/2}$, $^4F_{3/2} \rightarrow {}^4I_{11/2}$ and $^4F_{3/2} \rightarrow {}^4I_{13/2}$).

cannot be correlated with the order of vibrational frequency, suggests that structures of Nd(HFA-D)$_3$ in solution vary depending on solvent properties. One of the dominant processes for the quenching via vibrational excitation should be due to the O–D band ($\nu_{O\text{-}D} = 2500\ cm^{-1}$) of two coordinating D_2O molecules of Nd(HFA-D)$_3$ in solution. The effect of DMSO could be attributed to complete displacement of the coordinating D_2O molecules.

4. Luminescence of Nd(POM-D)$_3$

In order to prevent dipole–dipole energy transfer via cross relaxation through collisions between Nd^{3+} complex molecules, we successfully utilized deuterated bis-(perfluorooctanoylmethane); POM is a novel and bulky ligand (Fig. 6(b)). We now discuss the enhanced and characteristic emission of the tris(bis-(perfluorooctanoyl)methanato)neodymium(III), Nd(POM-D)$_3$, system in DMSO-d_6.

4.1. Luminescence in DMSO-d_6

Fig. 11 shows the absorption and luminescence spectra of DMSO-d_6 solutions (0.05M) of Nd(HFA-D)$_3$·2D$_2$O and Nd(POM-D)$_3$ determined under the same conditions and those of LHG-8 glass. Absorption is attributed to excitation from the ground state, $^4I_{9/2}$, to various excited-state levels. Both solution systems gave larger extinction coefficients than the glass system of LHG-8 (0.6 wt%).

Emission spectra were obtained by excitation at 585 nm ($^4I_{9/2} - {}^4G_{7/2}$). Emission peaks at 885, 1054 and 1325 nm were assigned to the f–f transitions of $^4F_{3/2} \rightarrow {}^4I_{9/2}$, $^4F_{3/2} \rightarrow {}^4I_{11/2}$ and $^4F_{3/2} \rightarrow {}^4I_{13/2}$, respectively. The full width at half maximum (FWHM) of the $^4F_{3/2} \rightarrow {}^4I_{11/2}$ transition was 25 nm, which is smaller than that of LHG-8 (35 nm) glass and that of Nd:YAG (30 nm). The shape of the emission band, which was more symmetrical and relatively narrower than that of LHG-8, suggests that the environment of Nd^{3+} in solution systems is at least as uniform as that in solid Nd^{3+} laser systems (Table 6).

4.2. Concentration-independent luminescence

To confirm the effect of the POM ligand which might prevent excitation migration even at collision between Nd^{3+} complexes, we measured the dependence of the

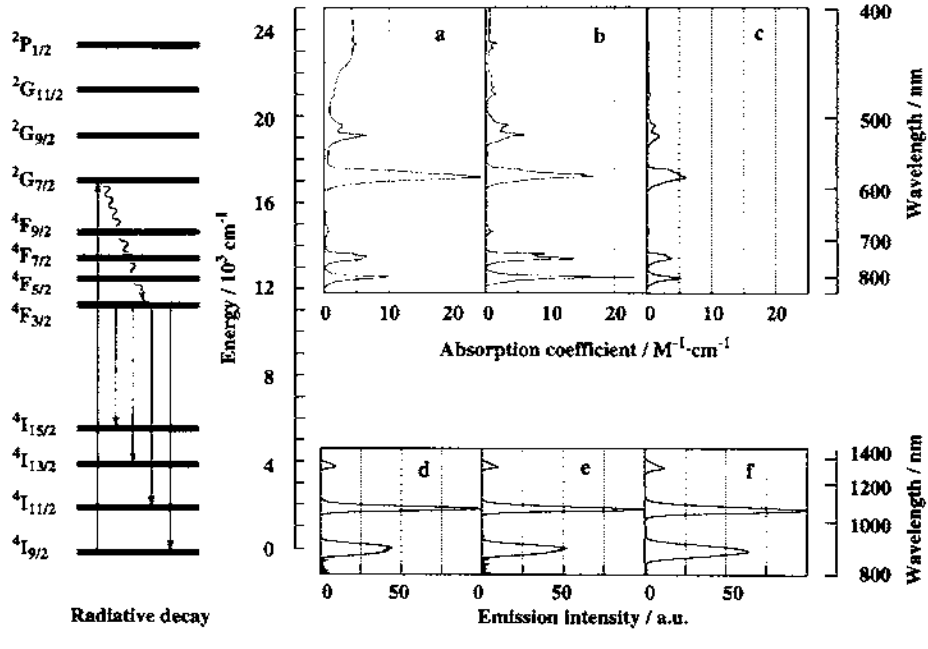

Fig. 11. Absorption and emission spectra of: (a,d) 0.1M Nd(HFA-D)$_3$ in DMSO-d_6, (b,e) 0.1M Nd(POM-D)$_3$ in DMSO-d_6 and (c,f) 0.6 wt% LHG-8.

emission efficiency on the concentration of Nd(POM-D)$_3$ in DMSO-d$_6$ and compared it with that in the Nd(HFA-D)$_3$ system.

The Nd(POM-D)$_3$ system has a higher quantum efficiency than the Nd(HFA-D)$_3$ system over the entire range of concentrations tested. While the quantum yield of Nd(HFA-D)$_3$ decreased as the concentration increased, that of the Nd(POM-D)$_3$ system was almost constant (3.2%) between 0.01 and 0.07M (Fig. 12).

According to the equation of the critical distance R_{DX} for nonradiative dipole–dipole energy transfer (Eq. (4)), the typical values of the critical distances for excitation migration ($^4F_{3/2}-{}^4I_{9/2}$) and cross-relaxation ($^4F_{3/2}-{}^4I_{15/2}$ and $^4I_{15/2}-{}^4I_{9/2}$) processes in the system of Nd^{3+}-containing phosphate laser glass were estimated to be 11.14 and 4.07 Å, respectively [29]. The emission decay $\tau(=W_{em}^{-1}$, emission rate) and quantum yield, η_{em}, of 0.1M Nd(HFA-D)$_3$ were 6.3 μs and 1.1%, respectively. Since the total spontaneous radiative emission rate is given by $A_r=\eta_{em}W_{em}$, the total spontaneous radiative emission rate of the present system is 1746 s^{-1} which is comparable to that of the Nd-containing glass ($A_r\cong 2400\ s^{-1}$). The absorption coefficient of Nd(HFA-D)$_3$ ($\epsilon=4.0M^{-1}\,cm^{-1}$) was also quite close to the value of Nd^{3+}-containing glass ($\epsilon=5.0M^{-1}\,cm^{-1}$) at 870 nm ($^4I_{9/2}\rightarrow{}^4F_{3/2}$ transition). According to Eq. (4), the critical distance of Nd(HFA-D)$_3$ was estimated as 11.7 Å.

In liquid systems, diffusional processes dominate energy transfer quenching [1]. The size of the Nd(HFA-D)$_3$ molecule is about 6 Å which is smaller than the critical distance (11.7 Å) of resonance energy transfer. The Nd(HFA-D)$_3$ complex could undergo collisional quenching with other Nd(HFA-D)$_3$ even at concentrations less than 0.1M (average distance between molecules in liquid media is estimated as 14 Å [30,31]).

In the system of Nd(POM-D)$_3$, the absorption coefficient was comparable to that of Nd(HFA-D)$_3$, and the quantum yield of Nd(POM-D)$_3$ was about three times larger than that of Nd(HFA-D)$_3$. From these results, the critical distance is estimated

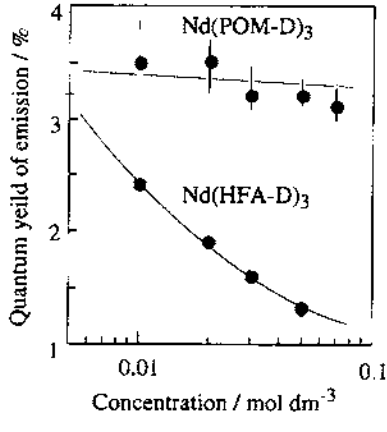

Fig. 12. Concentration dependence of quantum yield of Nd(HFA-D)$_3$ and Nd(POM-D)$_3$.

to be about 6 Å. The diameter of Nd(POM-D)$_3$, estimated by MM2, is 25 Å (CAChe ver. 6.10: Fig. 13), suggesting that the collision distance is much greater than 6 Å. Thus the distance should be enough to prevent excitation migration even at collision. The observed concentration-independent behavior of the quantum yield supports the hypothesis that excitation migration has been suppressed in the liquid system by the use of the bulky diketonato complex of Nd^{3+}.

4.3. Excitation migration at high concentration

A sudden decrease in the emission quantum yield of Nd(POM)$_3$ was observed at concentrations greater than 0.7M. Interestingly, dynamic light-scattering spectrophotometer (DLS) measurements showed an increase in the average size (102 Å) at a concentration of 0.4M (Fig. 14). The lipophobic perfluoroalkyl groups of Nd(POM)$_3$ should contribute to aggregation in DMSO, as is the case with surfactant molecules at the CMC in water.

The authors propose that Nd(POM)$_3$ aggregates at high concentrations and that this aggregation enhances energy transfer via an excitation hopping process, which leads to a decrease in the quantum yield of the luminescence. The high-order multipole and exchange interaction are also expected to contribute to the energy transfer process in such aggregated systems. The contributions of this process to the quenching are not clear at the present time [32].

The ratio of the emission intensity at 885 nm to that at 1053 nm reflects the

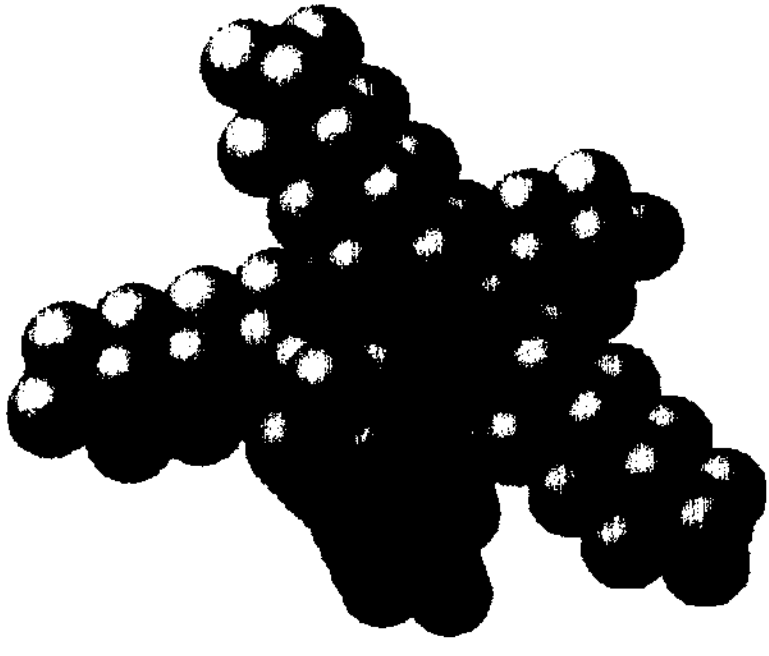

Fig. 13. Three-dimensional model of Nd(POM)$_3$ by MM2 calculation (CaChe system ver. 6.10).

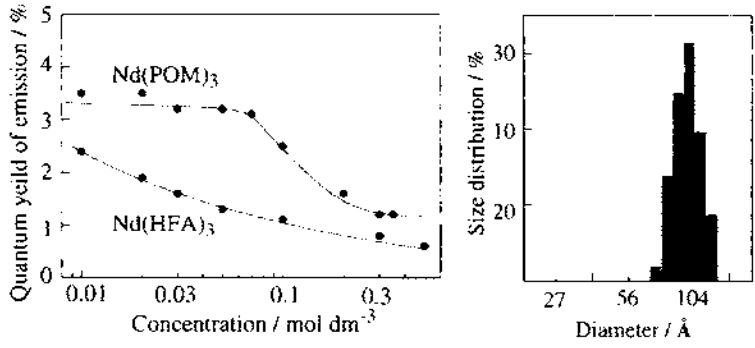

Fig. 14. The dependence of the quantum yields on the high concentration and size distribution of $Nd(POM)_3$ in DMSO determined by DLS measurements.

probability of excitation hopping between the complexes (excitation migration) [29]. When the emission at 885 nm is absorbed by a neighboring Nd^{3+} complex, the ratio changes because the re-absorbed light contributes to emission at 1054 nm. This ratio in the $Nd(POM\text{-}D)_3$ system was greater than that in the $Nd(HFA\text{-}D)_3$ system. This indicates that excitation migration in fluid solution is suppressed more in $Nd(POM\text{-}D)_3$ than in $Nd(NFA\text{-}D)_3$. Interestingly, this ratio in $Nd(POM\text{-}D)_3$ became smaller at the high concentration of 0.3M, suggesting excitation migration in the aggregated system. Dipole–dipole energy transfer between Nd^{3+} has been successfully suppressed in the liquid system by use of the bulky β-diketonato complex of Nd^{3+}.

5. Conclusion

The luminescence of the liquid Nd^{3+} system can be realized and enhanced by designing molecules which coordinate or solvate to Nd^{3+} in the system. Two kinds of deuterated β-diketone molecules, HFA-D and POM-D, containing C–F, C–O, O–D and C–D bonds, were found to bind Nd^{3+} and to enable the excited state ($^4F_{3/2}$) to undergo radiative relaxation, giving effective luminescence of Nd^{3+} in anhydrous deuterated organic solvents. Nonradiative relaxation via vibrational excitation and cross-relaxation processes could be suppressed effectively in the liquid systems.

The presence of D_2O in the Nd^{3+} primary coordination sphere contributes to nonradiative de-excitation and thus replacement of D_2O with solvent molecules with much lower vibrational bonds than D_2O could decrease the radiationless transition. The relatively weak emission of $[Nd(HFA\text{-}D)_3]\cdot 2D_2O$ in acetone-d_6 can be rationalized as due to the comparable coordination ability of acetone and D_2O. DMSO-d_6 molecules, which have higher electron density on the oxygen atom than D_2O molecules, can replace D_2O molecules. In other words, DMSO molecules alter the coordination structure of $Nd(HFA\text{-}D)_3$ in solution, and enhance the emission by

minimizing radiationless transitions via vibrational excitation because D_2O is eliminated from the vicinity of the Nd^{3+}.

The present luminescence enhancement is not sufficient for laser applications. Further effort is being directed towards designing ligands for Nd^{3+}. We seek to overcome the inherently low absorbance of neodymium. Asymmetric ligands and ligands with chromophores which absorbs light and transfer energy to Nd^{3+} seem promising for enhancing luminescence. The synthesis of such compounds is in progress and will be reported shortly.

Acknowledgements

The authors are very grateful to Dr. Tsuyoshi Asahi, Department of Applied Physics, Osaka University, for the emission lifetime measurements. The authors thank Dr. Yasushi Fujimoto for the quantum yield measurements and for his helpful comments.

References

[1] S. Hüfner, Optical Spectra of Transparent Rare Earth Compounds, Academic Press, New York, 1978, p. 208.
[2] M.J. Weber, Lanthanide and Actinide Chemistry and Spectroscopy, American Chemical Society, Washington, DC, 1980, p. 275.
[3] A.L. Schawlow, Springer Series in Optical Sciences, Laser, Spectroscopy and New Ideas, Springer-Verlag, New York, p. 47.
[4] Institute of Laser Engineering, Annual Progress Report, Osaka University, Osaka, 1995, 1996.
[5] K.A. Tanaka, T. Yamanaka, K. Nishihara, T. Norimatsu, N. Miyanaga, H. Shraga, M. Nakai, Y. Kodama, T. Kanabe, H. Azechi, M. Heya, T. Jitsuno, M. Kado, K. Miwa, M. Nakatsuka, A. Nishiguchi, H. Takabe, M. Takagi, K. Tsubakimoto, Y. Kato, Y. Izawa, S. Nakai, Phys. Plasmas 2 (1995) 2495.
[6] N.V. Rusakova, S.B. Meshkova, V.Ya. Venchikov, V.E. Pyatosin, M.P. Tsvirko, J. Appl. Spectrosc. (1992) 488.
[7] S.B. Meshkova, N.V. Rusakova, Z.M. Topilova, M.O. Lozinskii, L.S. Kudryavtesa, Koord. Khim. (1992) 210.
[8] A. Beeby, S. Faulkner, Chem. Phys. Lett. 266 (1997) 116.
[9] W. Siebrand, J. Chem. Phys. 46 (1967) 440.
[10] A. Heller, Appl. Phys. Lett. 9 (1966) 106.
[11] A. Heller, J. Am. Chem. Soc. 88 (1966) 2058.
[12] E.J. Schimitscheck, J. Appl. Phys. 39 (1968) 6120.
[13] M.N. Tolstoi, E.I. Lyubimov, I.M. Batyaev, Opt. and Spect. 28 (1970) 389.
[14] N. Blumenthal, C.B. Ellis, D. Grafstein, J. Chem. Phys. 48 (1968) 5726.
[15] C. Brecher, K.W. French, J. Phys. Chem. 73 (1969) 1785.
[16] T. Sasaki, T. Yamanaka, G. Yamaguchi, C. Yamanaka, Jpn. J. Appl. Phys. 8 (1969) 1037.
[17] M. Hongyo, T. Sasaki, Y. Nagao, K. Ueda, C. Yamanaka, IEEE J. Quant. Elect. 8 (1972) 192.
[18] Y. Hasegawa, K. Murakoshi, Y. Wada, S. Yanagida, J. Kim, N. Nakashima, T. Yamanaka, Chem. Phys. Lett. 248 (1996) 8.
[19] Y. Hawegawa, Y. Kimura, K. Murakoshi, Y. Wada, J. Kim, N. Nakashima, T. Yamanaka, S. Yanagida, J. Phys. Chem. 100 (1996) 10201.

[20] T. Förester, Organisher Verbindungen, Vandenhoeck and Ruprech, Göttingen, 1951.
[21] N. Mataga, T. Kubota, Molecular Interaction and Electronic Spectra, Marcel Dekker, New York, 1970.
[22] Y. Hasegawa, K. Murakoshi, Y. Wada, J. Kim, N. Nakashima, T. Yamanaka, S. Yanagida, Chem. Phys. Lett. 260 (1996) 173.
[23] M. Nakamura, R. Nakamura, K. Nagai, M. Shimoi, S. Tomoda, Y. Takeuchi, A. Ouchi, Bull. Chem. Soc. Jpn. 59 (1986) 332.
[24] R.C. Holz, L.C. Thompson, Inorg. Chem. 32 (1993) 5251.
[25] M. Sayeed, N. Ahmad, J. Inorg. Nucl. Chem. 43 (1981) 3197.
[26] K.L. Eckerle, W.H.V. Jr., V.R. Weidner, Appl. Opt. 15 (1976) 703.
[27] Y. Fujimoto, Rev. of Laser Eng. 25 (1997) 71.
[28] G.W. Burdick, C.K. Jayasankar, F.S. Richardson, Phys. Rev. B 50 (1994) 16309.
[29] J.A. Caird, A.J. Ramponi, P.R. Staver, J. Opt. Soc. Am. B8 (1991) 1391.
[30] F. Perrin, Ann. Chem. Phys. 17 (1932) 283.
[31] C. Gösele, M. Hauser, U.K.A. Klein, R. Frey, Chem. Phys. Lett. 34 (1975) 519.
[32] M. Burton, J.J. Kirby-Smith, J.L. Maggee, Comparative Effect of Radiation, Wiley, New York, 1960.